A Review on Noise Estimation Methods in Multi-coil MRI

[1]Soumya V, [2]Abraham Varghese, [3]Neetha N
[1,2,3]Department of Computer Science and Engineering
Adi Shankara Institute of Engineering and Technology, Ernakulam, India
Email: [1]soumyav17@gmail.com, [2]abrahamvarghese77@gmail.com

***Abstract*—Noise in an image is variation of information from the actual data. If there is any noise in the medical image then consequence will be huge. Physician won't be able to do proper diagnose of the disease and can also affects the quality of post processing techniques like registration and segmentation. Modern techniques use multiple coil MRI(Magnetic Resonance Imaging) where noise varies with position in the image i.e., non-stationary noise. Many methods are available for the non-stationary noise estimation in the literature but those needs multiple acquisitions and additional details. These limitations are avoided in homomorphic approach. Aja-Fernandez et.al used homomorphic approach on Devore et al. and is found to be a good method. In this paper homomorphic approach is applied on different known noise estimation methods in multi-coil MRI and a comparison is made. Visual comparison and quantitative analysis shows that homomorphic approach on Devore et.al gives better result for both Gausssian and Rician than other methods.**

***Index Terms*—multi-coil MRI; noise estimation; Rician; non-central chi(nc-χ) distribution**

I. Introduction

Noise can arise during image acquisition or during image transmission. It is the unwanted information that comes along with the useful information or rather it can be defined as variation of the data from the actual data present in the image. Medical images like CT, MRI, and ultrasound having noise will reduce the visual clarity and hence will cause incorrect diagnosis of the disease. In MRI, noise can arise from movement of the patients, eddy current losses in patient, number of scanning times and restrictions in hardware[2].

Lots of literature study has been already done on the noise estimation of noise for single coil MRI. In the picture domain, it is considered noise will have zero mean and spatially uncorrelated Gaussian procedure[3]. The real and imaginary parts will have equal variance. So noise will have stationary noise distribution and magnitude signal follows a Rican distribution. The major disadvantage for the single coil is its scanning time.

In the case of multi-coil MRI, multiple images are acquired simultaneously and they are combined to get the final image. The main advantage over here compared to single coil is the scanning time reduction. Modern techniques like parallel acquisition techniques for example, Generalized Auto calibrating Partially Parallel Acquisitions(GRAPPA) or Sensitivity Encoding(SENSE) are uses multi-coil mechanism in order to decrease the scanning time and to improve the visual quality. In these techniques multiple images are acquired simultaneously instead of acquiring image sequentially as in the case of single coil. The noise distribution will be non-stationary where noise characteristics will be different for each and every location in MRI. Noise model used for MRI are Rician and nc-χ distribution.

Noise is one of the main challenge in the medical imaging field which affects the image enhancement and other post processing. Main objective of this work is to apply homomorphic approach on different methods and compare these methods so that best techniques can be derived that can effectively estimate noise in multi-coil MRI so that it will be helpful to denoise MRI more accurately and can be useful for post processing like registration, segmentation and also for correct diagnosis of the disease.

In Sections II, gives a glimpse on multi-coil MRI and related work on noise estimation techniques, section III explains the theory behind proposed method. In Section IV, experiments and results are discussed. Finally, conclusions are drawn in Section V.

II. Multi-coil MRI

In order to get the final image for multi-coil MRI, there needs to combine images from numerous coil. Here the noise characteristics will vary with each every pixel in the image. Key benefit while considering multi-coil is higher Signal to Noise Ratio(SNR) and in less scanning time. Multi-coil can be speeded by Parallel MRI(pMRI) technique.

Consider, there are i number of coils antenna configured in the system. The complex signal, $S_i(x)$ obtained from i^{th} coil after inverse Fourier transform can be represented as [4]:

$$S_i(x) = T_i(x) + N_i(x;\sigma_i^2) \tag{1}$$

where $T_i(x)$ is the noise free complex signal for each coil i (for i=1, 2,, I) and the complex Gaussian noise in each coil can be expressed as:

$$N_i(x;\sigma_i^2) = N_{ir}(x;\sigma_i^2) + jN_{ii}(x;\sigma_i^2). \tag{2}$$

Here $N_{ir}(x;\sigma_i^2)$ is the real part and $jN_{ii}(x;\sigma_i^2)$ is imaginary part. The ultimate resulted image will be influenced by the technique utilized to combine the information of multi-coil into single image. Sum-of-squares(SoS) is used to avoid additional details. Now the composite magnitude signal for the coils i, ranging from 1 to I can be expressed as[1,3]:

$$M(x) = \Sigma|S_i(x)|^2 \tag{3}$$

A. Noise Estimation

Multi-coil MRI follows non-stationary noise distribution and so there needs to be taken care of noise estimation for spatially variant noise map. There are many non-stationary noise estimation methods available in the MRI literature.

Devore et al.[1,5] have used expectation-maximization(EM) algorithm to evaluate of maximum likelihood of Rician distribution parameters from training data. Authors have used EM algorithm for finding non-homogeneous noise in Rician data. This method uses several sample data from the receiver signal.

Samsonov and Johnson[6] used details of MRI noise level in spatial distribution from receiver coil and consumed for fine-tuning anisotropic diffusion filter. Sometimes theses noise information is may not be obtainable in clinics.

Goosens et al.[7] have assumed that image is corrupted with non-stationary additive white Gaussian noise. Local noise variance for each pixel is assessed from local square window surrounding this pixel. Wavelet domain method is used for noise estimation in the image. They have used highest frequency sub-band assuming for high noise levels, this sub-band comprises noise. Rician data is not considered here so this cannot be used for MRI denoising.

Delakis et al.[1,8] generated noise map for finest scale by taking inverse wavelet transform and direct analysis. Edge pixels are removed and then local noise variance estimated from wavelet high frequency sub-band. In this approach signal components are suppressed to determine the spatially variant noise. Rician noise distribution is not measured in this method.

Landman et al.[9] have estimated spatially variable noise fields based on Q_n estimator. Then regularization is applied using coil sensitivity model for improving the robustness against artefacts.

Guo et al.[10] Have recommended local mutual information and k-means segmentation to get the edge information and local variance is used to extract the noise distribution in other regions.

Ding et al.[11] have recommended local mutual information and k-means segmentation to get the edge information and local variance is used to extract the noise distribution in other regions. Edge overestimation is the main disadvantage of this technique and mathematical morphology filter is used to overcome this.

Manjon et al.[12] estimated noise variance by taking smallest distance of neighborhood pixel around the required pixel. They use non-local means filter by taking weighted average of neighborhood pixels and repairs every pixels. Here Rician distribution is taken into account for non-stationary noise. Main advantage of the suggested method is it doesn't want extra parameter for the noise level. But this method require Signal to Noise ratio(SNR) iterative estimation.

Maximov et al.[13] noise is estimated with the help of MAD estimator[14]. Here noise is measured pixel by pixel. Then correction factor is applied for each pixel. Low and high SNR has been taken care for Rician noise distribution. SNR estimation is required in this method.

Liu et al. [1,15] have extended of MAD estimator and estimated spatially varying noise standard deviation (σ) in the wavelet domain. Then is corrected for each pixel.

III. Methods Used

Homomorphic methodology proposed by Aja-Fernandez et al.[1] is used here. It is considered that spatially dependent variance $\sigma^2(x)$ is low pass signal. Noise maps are extracted for three cases like Gaussian, Rician and Rayleigh. Aja-Fernandez used homomorphic approach on the method proposed in Devore et al.[5].

Gaussian noise estimation is done by following the series of steps. First mean of the image deducted from the image then logarithm applied, followed by low pass filtering and later exponential is taken on the result to obtain the estimator.

Rayleigh noise estimation is done by applying logarithm and then low pass filtering on the result of first step. Followed by taking exponential to obtain the estimator.

Rician noise estimation is done by first removing the local mean from the image and then logarithm is applied and followed by low pass filtering. Later expected value is determined to obtain the estimator.

In this paper homomorphic approach is applied on different known noise estimation methods in multi-coil MRI and a comparison is made. The methods used for estimation of non-stationary noise in MRI includes Devore et al.[5], Goosens et al.[7], Delakis et al.[8], Manjon et al.[12], Maximov et al.[13], Liu et al.[15].

IV. Experiments and Results

Synthetic experiments are conducted on Brainweb database[16], [19]. Firstly noise free MRI is taken from brainweb[19]. Noise maps are generated artificially [2] by adding noise to the original MRI from brainweb. Since multi-coil has Slice of MRI corrupted by non-stationary Rician noise is created by adding noise map. And from the magnitude MRI noise map is measured. Fig. 1 demonstrates the input images with noise free MRI, noise map and non-stationary noisy MRI. To create Non-stationary noise, noise map is

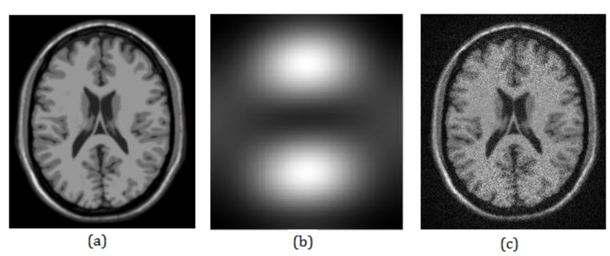

Fig. 1. (a)Noise free MRI (b)Noise map (c)Non-stationary noisy MRI.

added into the noise free MRI along with random noise. Homomorphic approach is employed to remove noise from non-stationary MR data. Two scenarios has been considered here, i.e. for Gaussian and Rician. In the case of Gaussian scenario, two filters are being utilized for evaluating the noise map and stationary component. Filter for low pass to attain the noise map $\sigma(x)$ and filter for high pass filter get the stationary noise part N(x).

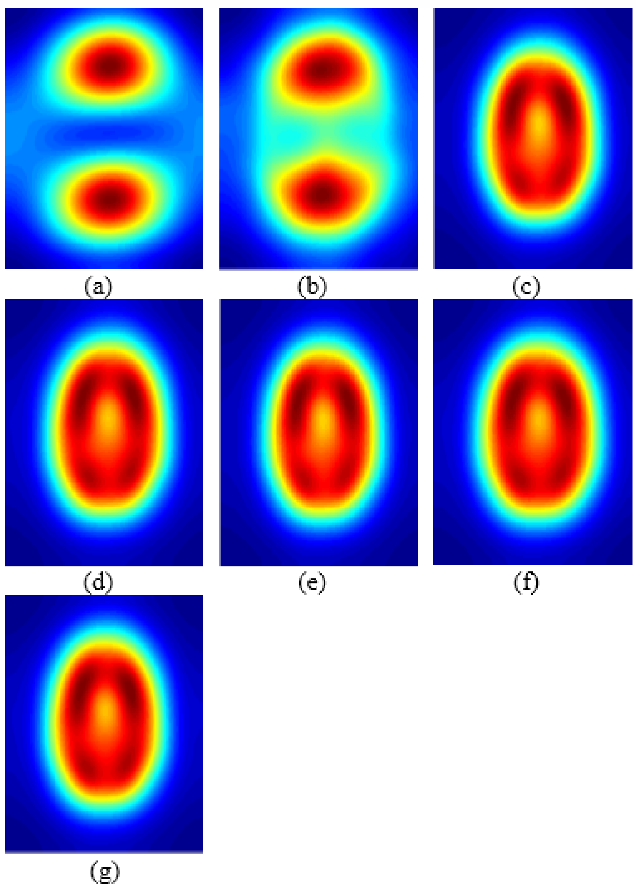

Fig. 2. Noise Estimation for Rician case (a)Original noise map (b)Devore (c)Goossens (d)Delakis (e)Liu (f)Maximov (g)Manjon.

Original noise map is compared with methods like Devore, Goossens, Delakis, Liu, Maximov, Manjon after applying homomorphic approach for both Rician and Gaussian case. From the visual comparison of fig.2 and fig.3, it is clear that homomorphic approach on Devore method shows better results than others.

Quantitative analysis is done based on the Maximum value of error, minimum value of error and Structural Similarity Index Measure(SSIM). Structural similarity is based on the verification between original noise map with noise map result of different homomorphic approach.

Homomorphic approach on Devore shows least value for Maximum value of error, Mean value of error for both Rician and Gaussian case. While taking structural similarity index measure for Rician case homomorphic approach on Devore,Goosens and Liu shows highest similarity with original noise map. In the case of structural similarity index measure for Gaussian case Homomorphic approach on Devore shows highest similarity with original noise map.

Maximum value of error can be calculated by taking the maximum value of difference between original noise map and estmated noise map. Original noise map depicted in Fig. 1 and

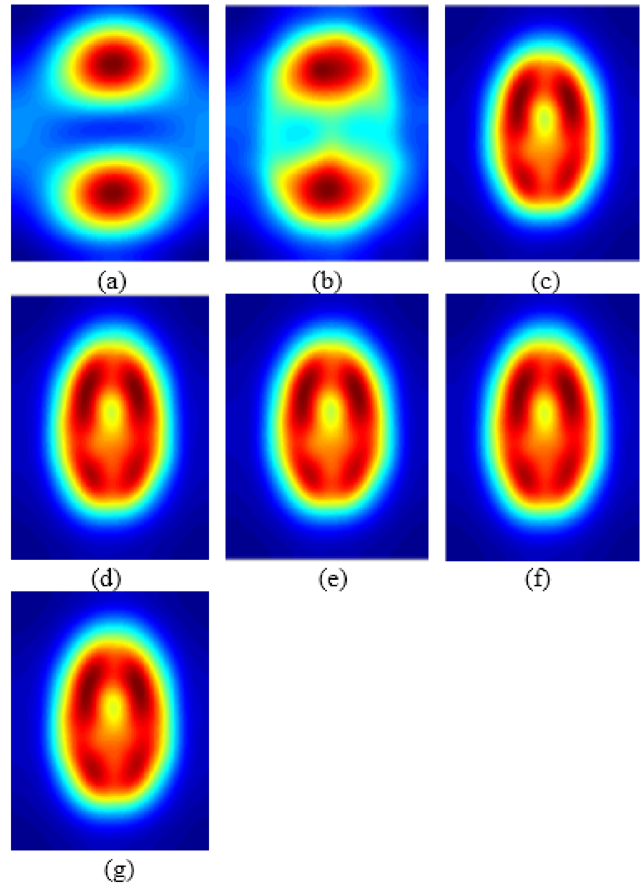

Fig. 3. Noise Estimation for Gaussian case (a)Original noise map (b)Devore (c)Goossens (d)Delakis (e)Liu (f)Maximov (g)Manjon.

the estimated noise map measured using each method after applying homomorphic approach as depicted in Fig. 2., in the case of Rician and Fig. 3., in the case of Gaussian. This can be represented as:

$$Max.error = |Map1 - Map2|Max \tag{4}$$

Where Max. error is the Maximum value of error, Map1 is the original noise map and Map2 is the estimated noise map estimated by using different homomorphic methods. Fig. 4 depicts maximum value of error for Rician case and Devore shows better result. Fig. 5 shows maximum value of error for Gaussian case and Devore shows better result.

Mean value of error is calculated by taking average of the difference between the original noise map and the estimated noise map. This can be represented as:

$$Mean.Error = \Sigma\sigma(Map1 - Map2)/n \tag{5}$$

Where Mean. error is the Mean value of error, Map1 is the original noise map(Map1) depicted in Fig. 1 and Map2 is the noise map depicted in Fig. 2., in the case of Rician and Fig. 3., in the case of Gaussian and n represents the total number of elements. Fig. 6 depicts mean value of error for Rician case and Devore shows better result. Fig. 7 depicts mean value of error for Gaussian case and Devore shows better result.

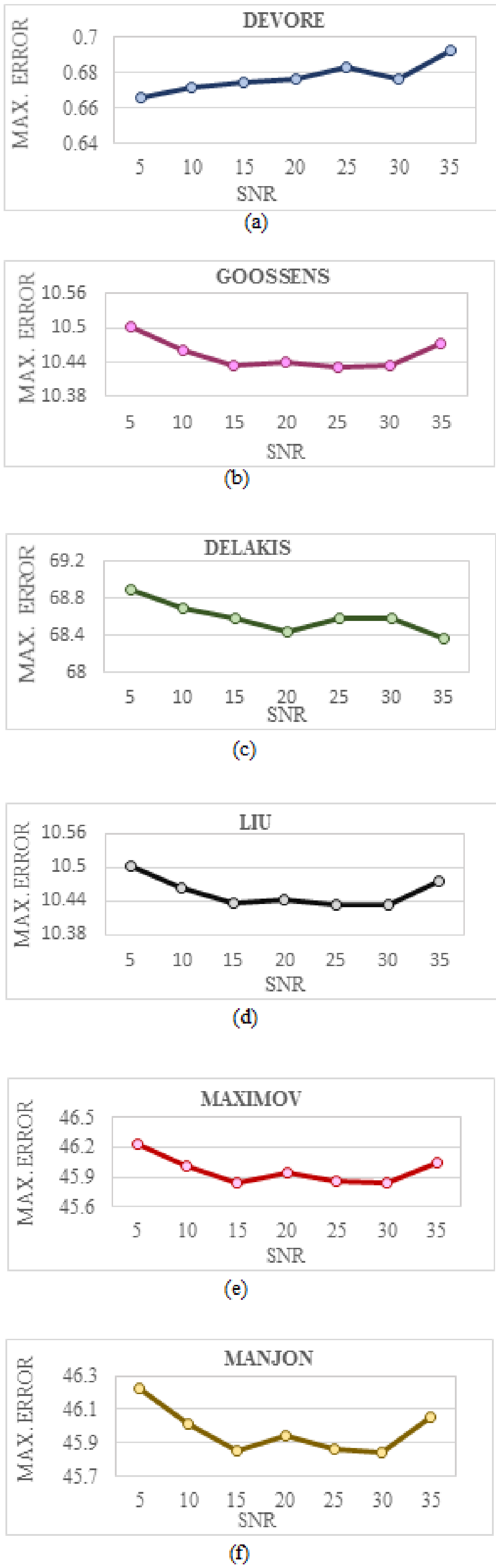

Fig. 4. Maximum value of error for Rician case: (a)Devore (b)Goosens (c)Delakis (d)Liu (e)Maximov (f)Manjon.

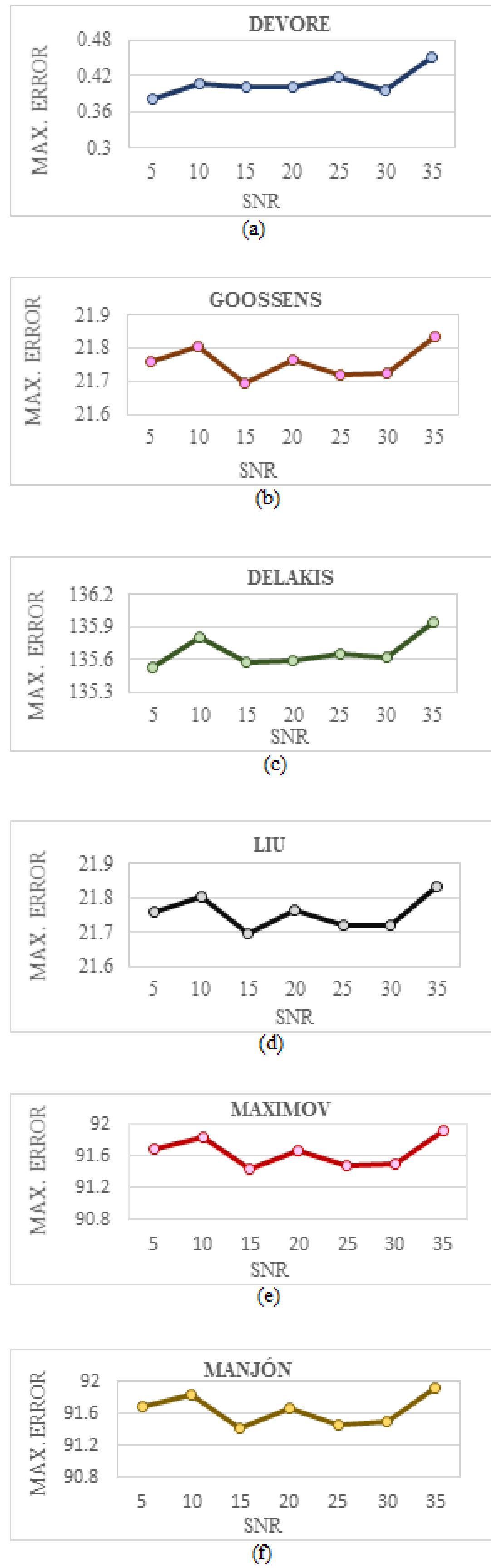

Fig. 5. Maximum value of error for Gaussian case: (a)Devore (b) Goosens (c)Delakis (d)Liu (e)Maximov (f)Manjon.

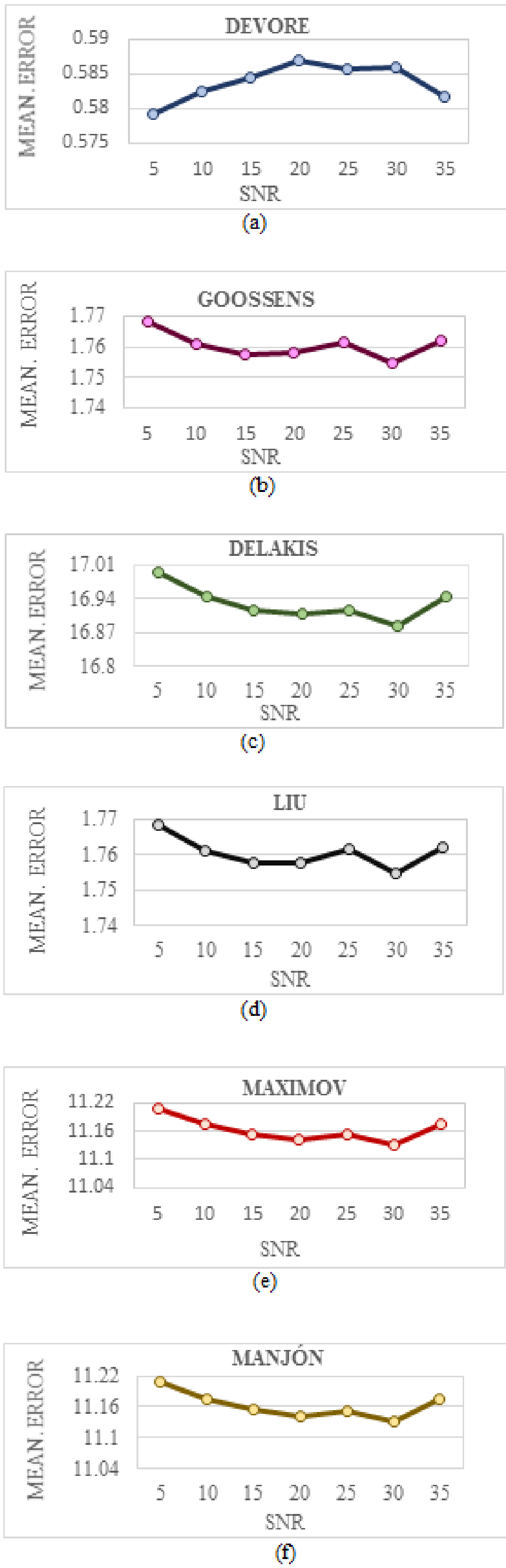

Fig. 6. Mean value of error for Rician case: (a)Devore (b)Goosens (c)Delakis (d)Liu (e)Maximov (f)Manjon.

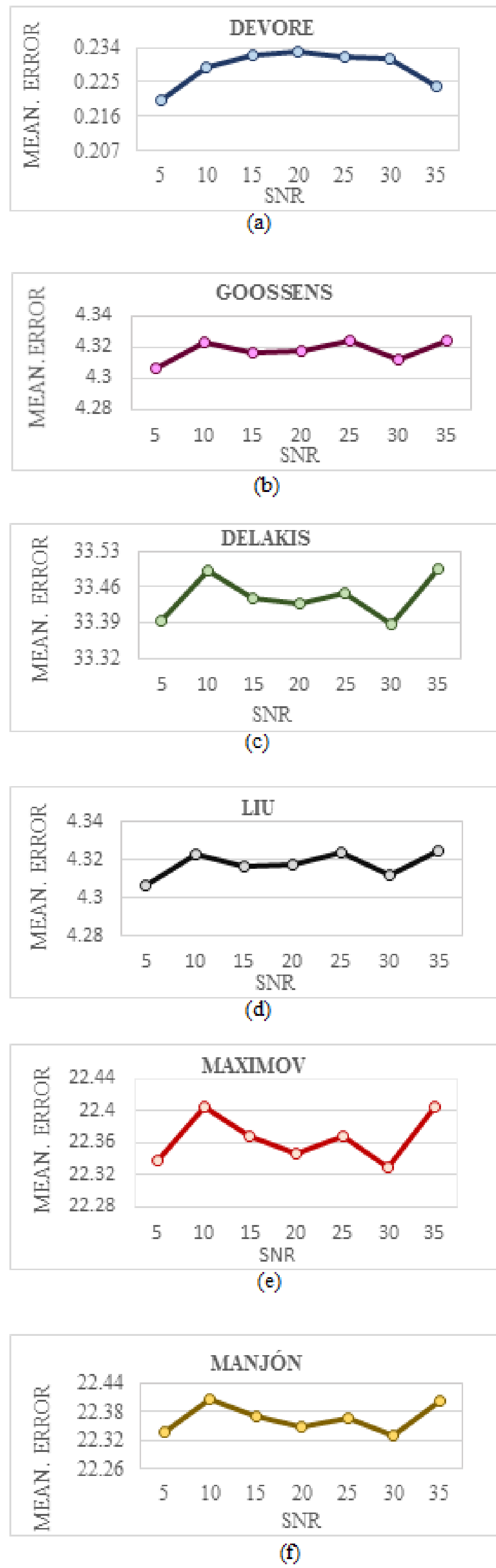

Fig. 7. Mean value of error for Gaussian case: (a)Devore (b)Goosens (c)Delakis (d)Liu (e)Maximov (f)Manjon

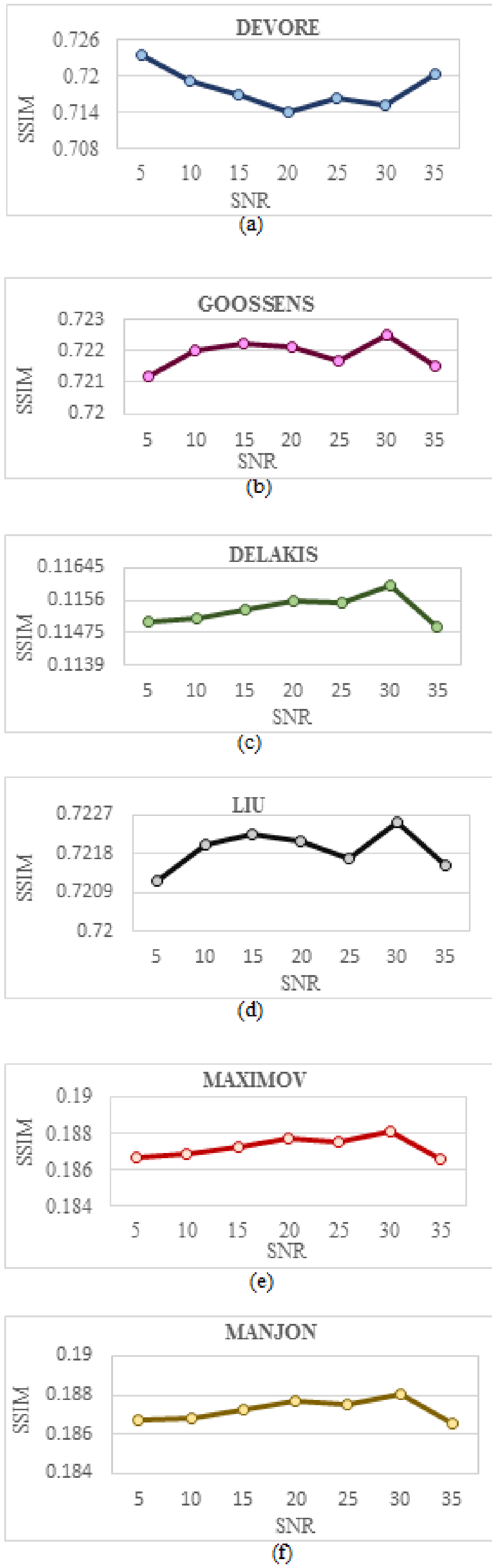

Fig. 8. Structural similarity index for Rician case: (a)Devore (b)Goosens (c)Delakis (d)Liu (e)Maximov (f)Manjon

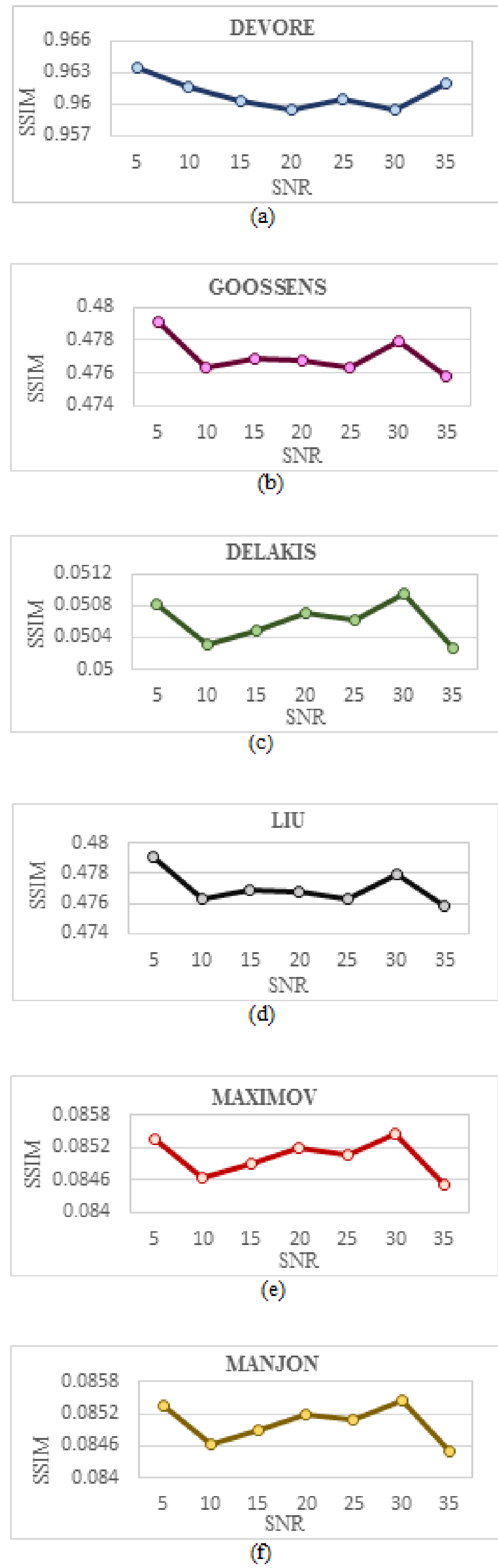

Fig. 9. Structural similarity index for Gaussian case: (a)Devore (b)Goosens (c)Delakis (d)Liu (e)Maximov (f)Manjon

SSIM is measured by verifying the difference in terms of structural information between Map1 and Map2. Where Map1 is the original noise map depicted in Fig. 1 and Map2 is the noise map depicted in Fig. 2., in the case of Rician and Fig. 3., in the case of Gaussian. Fig. 8 depicts SSIM for Rician case and Devore shows better similarity. Fig. 9 depicts Structural similarity index for Gaussian case and Devore shows better similarity. From the visual comparison it is clear that Homomorphic approach on Devore shows better result for both Gausssian and Rician. In the case of Quantitative result for similarity index measure for Rician case, homomorphic approach on Devore, Goosens and Liu shows better similarity with original noise map. Homomorphic approach on Devore shows highest similarity with original noise map for Gaussian case.

V. Conclusion

In this paper homomorphic approach is applied on different known noise estimation methods in multi-coil MRI like Devore et al.[5], Goosens et al.[7], Delakis et al.[8], Manjon et al.[12], Maximov et al.[13] and a comparison is made. Here multi-coil MRI with Rician and Gaussian noise distributions are considered. Visual comparison shows that homomorphic approach on Devore gives better result for both Gausssian and Rician than other methods. Quantitative analysis is done based on maximum value of error, mean value of error and SSIM and Devore after applying homomorphic shows better result for both Gausssian and Rician.

Appendix A
Devore et al.[5]

For a single MRI, parameters for maximum likelihood estimates β and σ^2 can be calculated as:

$$\beta_{k+1}(x) = \left\langle \frac{I_1\left(\frac{\beta_k(x)I(x)}{\sigma_k^2(x)}\right)}{I_0\left(\frac{\beta_k(x)I(x}{\sigma_k^2(x)}\right)} I(x) \right\rangle_x \tag{6}$$

$$\sigma_{k+1}^2(x) = max\left\{\frac{1}{2}\left\langle I^2(x)\right\rangle_x - \frac{(\beta_k(x))^2}{2}, 0\right\} \tag{7}$$

Here $I_n(.)$ is the modified Bessel function of 1st kind and n^{th} order and k is the number of iteration. For initialization method of moments is used and can be given as:

$$\beta_0 = \left\{2\left(\frac{1}{n}\sum_{j=1}^{n} r_j^2\right)^2 - \frac{1}{n}\sum_{j=1}^{n} r_j^4\right\}^{\frac{1}{4}} \tag{8}$$

$$\sigma_0^2 = \frac{1}{2}\left(\frac{1}{n}\sum_{j=1}^{n} r_j^2 - \beta_0^2\right) \tag{9}$$

$$SNR = \frac{\beta_k(x)}{\sigma_k(x)} \tag{10}$$

local sample estimator of the mean is given as:

$$\langle I(x)\rangle_x = \frac{1}{|\eta(x)|}\sum_{p\epsilon\eta(x)} I(p) \tag{11}$$

where $\eta(x)$ neighborhood centered in x.

Appendix B
Goossens et al.[7]

The estimator can be given as:

$$\sigma^2(x) = \left\langle \left(I^{(1,HH)}(x)\right)^2 \right\rangle_x \tag{12}$$

where $I^{(1,HH)}(x)$ is high high sub band coefficients of the Stationary Wavelet Transform(SWT) and $\langle I(x)\rangle_x$ is the local sample estimator of the mean.

Appendix C
Delakis et al.[8]

The estimator can be given as:

$$\sigma^2(x) = \left(2 - \frac{\Pi}{2}\right)^{-1}\left[\left\langle \tilde{i}^2(x)\right\rangle_x - \left(\left\langle \tilde{i}(x)\right\rangle_x\right)^2\right] \tag{13}$$

where $\tilde{i}(x)$is the image with high frequency after removing low low sub band through SWT.

Appendix D
Manjon et al.[12]

The estimator can be given as:

$$\sigma^2(x) =_{p\epsilon\eta(x):p\neq x}^{min} \|R(x) - R(p)\|_2^2 \tag{14}$$

where R(x)=I(x)- $\psi(I(x))$ and $\psi(I(x))$ having low pass filtered data. For low SNR, a correction is done as:

$$\sigma_1(x) = \frac{\sigma(x)}{\sqrt{\xi(\theta)}} \tag{15}$$

$\xi(\theta)$ is the function [18] and θ is calculated iteratively and can be shown as:

$$\theta_{k+1} = \sqrt{\xi(\theta_k)\left(1 + \frac{\langle I(x)\rangle_x^2}{\sigma^2(x)}\right) - 2} \tag{16}$$

Appendix E
Maximov et al.[13]

The estimator can be given as:

$$\sigma(x) = 1.4826 MAD_x(I(x)) \tag{17}$$

Here σ(x) is the Gaussian estimator and correction is required for low SNR.

Appendix F
Liu et al.[15]

The estimator can be given as:

$$\sigma(x) = 1.4826 MAD_x(I^{(1,HH)}(x)) \tag{18}$$

$MAD_x(.)$ is local median absolute deviation can be expressed as:

$$MAD_x(I(x)) =_{median_{p\epsilon\eta(x)}} |I(p) median_{q\epsilon\eta(x)}(I(q))| \tag{19}$$

where $I^((1,HH))$ is the High high subband coefficients of SWT of I(x). Correction for low SNR can be applied using Eq. (15)

Acknowledgment

The authors would like to thank Dr Santiago Aja-Fernndez, Associate Professor, university of Valladolid, Spain for his valuable discussions, timely suggestions on multi-coil MRI noise estimation also for providing information about the multi-coil MRI.

References

[1] S. Aja-Fernández, T. Pieciak, G. Vegas-Sánchez-Ferrero and others, ”Spatially variant noise estimation in MRI: A homomorphic approach,” *Medical image analysis*, vol. 20, no. 1, pp. 184–197, 2015.

[2] S. Aja-Fernández, G. Vegas-Sánchez-Ferrero and A. Tristán-Vega, ”Noise estimation in parallel MRI: GRAPPA and SENSE,” *Magnetic resonance imaging*, vol. 32, no. 3, pp. 281–290, 2014.

[3] S. Aja-Fernández and A. Tristán-Vega, ”A review on statistical noise models for Magnetic Resonance Imaging,” *LPI, ETSI Telecomunicacion, Universidad de Valladolid, Spain, Tech. Rep*, 2013.

[4] S. Aja-Fernández, A. Tristán-Vega and C. Alberola-López, ”Noise estimation in single-and multiple-coil magnetic resonance data based on statistical models,” *Magnetic resonance imaging*, vol. 27, no. 10, pp. 1397–1409, 2009.

[5] M.D. DeVore, A.D. Lanterman and J.A. O'Sullivan, ”ATR performance of a Rician model for SAR images,” *AeroSense 2000*, pp. 34-45, 2000.

[6] A. A. Samsonov, and C. R. Johnson, ”Noise-adaptive nonlinear difusion fltering of MR images with spatially varying noise levels,” *Magnetic Resonance in Medicine*, vol. 52, no. 4, pp. 798-806, 2004.

[7] B. Goossens, A. Pizurica, and W. Philips, ”Wavelet domain image denoising for non-stationary noise and signal-dependent noise,” *Image Processing, 2006 IEEE International Conference on*, pp. 1425-1428, 2006.

[8] I. Delakis, O. Hammad, and R. I. Kitney, ”Wavelet-based de-noising algorithm for images acquired with parallel magnetic resonance imaging (MRI),” *Physics in Medicine and biology*, vol. 52, no. 13, pp. 3741, 2007.

[9] B. A. Landman, P.-L. Bazin, S. A. Smith, and J. L. Prince, ”Robust estimation of spatially variable noise fields,” *Magnetic Resonance in Medicine*, vol. 62, no. 2, pp. 500-509, 2009.

[10] W. Guo and F. Huang, ”Adaptive total variation based filtering for MRI images with spatially inhomogeneous noise and artifacts,” *Biomedical Imaging: From Nano to Macro, 2009. ISBI'09. IEEE International Symposium on*, pp. 101-104, 2009.

[11] Ding, Yu, YiuCho Chung, and Orlando P. Simonetti. ”A method to assess spatially variant noise in dynamic MR image series,” *Magnetic Resonance in Medicine*, vol. 63, no. 3, pp. 782-789, 2010.

[12] J.V. Manjón, P. Coupé, L. Martí-Bonmatí, D.L. Collins and M. Robles, ”Adaptive non-local means denoising of MR images with spatially varying noise levels,” *Journal of Magnetic Resonance Imaging*, vol. 31, no. 10, pp. 192-203, 2010.

[13] I. I. Maximov, E. Farrher, F. Grinberg, and N. J. Shah, ”Spatially variable Rician noise in magnetic resonance imaging,” *Medical image analysis*, vol. 16, no. 2, pp. 536-548, 2012.

[14] P. Coupé, J.V. Manjón, E. Gedamu, D. Arnold, M. Robles and D.L Collins, ”Robust Rician noise estimation for MR images,” *Medical image analysis*, vol. 14, no. 4, pp. 483–493, 2010.

[15] R. W. Liu, L. Shi, W. Huang, J. Xu, S. C. H. Yu, and D. Wang, ”Generalized total variation-based MRI Rician denoising model with spatially adaptive regularization parameters,” *Magnetic resonance imaging*, vol. 32, no. 6, pp. 702-720, 2014.

[16] D. L. Collins, A. P. Zijdenbos, V. Kollokian, J. G. Sled, N. J. Kabani, C. J. Holmes, and A. C. Evans, ”Design and construction of a realistic digital brain phantom,” *Medical Imaging*, IEEE Transactions on, vol. 17, no. 3, pp. 463-468, 1998.

[17] P.J. Rousseeuw and C. Croux, ”Journal of the American Statistical association,” *Journal of the American Statistical association*, vol. 88, no. 424, pp. 1273–1283, 1993.

[18] C. G. Koay and P. J. Basser, ”Analytically exact correction scheme for signal extraction from noisy magnitude MR signals,” *Journal of Magnetic Resonance*, vol. 179, no. 2, pp. 317-322, 2006.

[19] BrainWeb: Simulated Brain Database ”http://brainweb.bic.mni.mcgill.ca/brainweb/”